

AD720090

ROYAL AIRCRAFT ESTABLISHMENT

Technical Report 70106

June 1970

THE EFFECT OF HUMIDITY ON A CORONA DISCHARGE IN AIR

by

B. R. Maskell

SUMMARY

The effect of humidity on a corona discharge in air is investigated and found to produce a decrease in discharge current of about 20% for a change in humidity from dry to saturated conditions at atmospheric pressure and room temperature. It is suggested that this effect can be used to measure humidity in applications where rapid response is essential and the need to compensate for moderate temperature and pressure changes can be tolerated.

Departmental Reference: I & R 113

CONTENTS

	<u>Page</u>	
1 INTRODUCTION	3	-
2 THE CORONA DISCHARGE	4	.
3 EXPERIMENTAL DETAILS	6	
4 RESULTS	8	
4.1 Comparison with theory	8	
4.2 The effect of humidity	9	
4.3 The effect of temperature	9	
4.4 The effect of pressure	9	
4.5 Polarity	10	
5 DISCUSSION AND CONCLUSION	10	
Appendix A The current-voltage relation	13	
Appendix B Offset voltage and plotter sensitivity	16	
References	17	
Illustrations	Figures 1-9	
Detachable abstract cards	-	

1 INTRODUCTION

Corona is a glow discharge occurring at atmospheric pressures in the small region of high electric field strength surrounding sharply curved conductors. It has been the subject of considerable study^{1,2}, both in its own right and as a means of investigating the mechanisms present in uniform field discharges. The effect of water vapour on a corona discharge has however received comparatively little attention, the main body of investigation being restricted to measurements of power loss from high voltage transmission lines in the open air³. In such studies it is difficult to isolate the effect of water vapour from that of water droplets either on the wire or in the air⁴.

The object of this investigation was to study the influence of water vapour on corona discharge current and to assess the value of this effect as a means of measuring humidity. It is reasonable to expect that a humidity meter based on such an effect would have a rapid response which, combined with a wide humidity range, would give it a potential advantage for some applications over many of the instruments in current use.

One of the earliest methods of humidity measurement was the determination of dew point by cooling a surface until dew appears. The automated and reasonably compact devices currently available have been made possible, at the expense of electronic complexity, by the use of thermoelectric coolers⁵, but these do not significantly improve the response time which is limited by the cooling rate attainable. The minimum temperature that can be reached is also dependent on cooling rate, and this imposes a lower limit on the range of the device. Jury et al.⁶ have attempted to produce a fast-response device, but with limited success.

The use of hygroscopic materials has also enjoyed a long-standing prominence in this field. The amount of water absorbed or adsorbed by these substances is detected by a change in dimension, weight or electrical properties. Devices relying on this principle are limited in rate of response by the speed of the sorption or desorption process, but by reducing the size of the sensor, response times can also be reduced. Lai and Hidy⁷ have produced a microsensor with a response time of about 100 ms but it is relatively insensitive at less than 30% RH. Alternatively thin films of hygroscopic material have been employed in an attempt to increase the response rate. Jason⁸ has used an aluminium oxide film and monitored the resistance and capacitance between the base of an anodized plate and a porous aluminium film deposited onto the exposed outside surface. Again there is a decrease in sensitivity at low humidity, and the response time is about 1 second.

The need for a porous electrode can be eliminated by measuring the mass of water in the film through its effect on the frequency of a quartz crystal oscillator upon which the hygroscopic film is deposited. Gjessing et al.⁹ have produced a device of this type which responds to humidity changes up to 50 Hz and, with suitable choice of materials, in an almost linear fashion from about 15% to 95% RH.

Humidity in air has also been measured by more direct processes. Sargent¹⁰ has described a method of measuring the refractive index of air, which can be related to water vapour pressure, using microwave techniques. The response of the basic hygrometer is limited by the rate at which the servo-system can respond to stabilise the resonant frequency of a test cavity. However, to eliminate temperature effects, both test and reference cavities and air samples are maintained at 45°C with consequential deterioration in response.

The problem of temperature effects is not encountered when dealing with spectroscopic hygrometry. An infra-red absorption hygrometer which compares the attenuation in 30 cm long beams of 2.45 μm and 2.60 μm wavelength radiation has been reported by Wood¹¹. It is limited in response only by the rate of sampling between the beams (60 Hz) and the speed of the servo-mechanism employed to adjust the initial intensities of the beams differentially, maintaining a null output.

It is suggested that the corona discharge can be employed as a hygrometer with a performance comparable to the microwave device referred to above, viz. it will have a wide range and rapid response but will be subject to side effects; however it has the additional advantage of simplicity and low cost.

The existing theory of corona discharge is briefly reviewed in section 2, together with some early empirical expressions for onset voltage and current-voltage characteristics. On the basis of these relations the chamber described in section 3 was designed in which a corona discharge cell can be subjected to a variety of conditions of temperature, pressure and humidity. The results obtained are presented in section 4 and in section 5, suggestions are made about the possible applications of the effect.

2 THE CORONA DISCHARGE

A corona discharge differs from a uniform field discharge in that one (or both) of its electrodes exhibits sharp curvature, and breakdown occurs first in the high field region surrounding this electrode. The electric field in the remainder of the gap is of much smaller magnitude and thus prevents the complete breakdown to a spark.

Several electrode configurations will produce this type of discharge, but the most convenient, from both theoretical and experimental points of view, is a coaxial cylindrical system. We shall therefore confine our attention to such an arrangement in which the radius of the inner cylinder (or wire) is much smaller than that of the outer cylinder.

The mechanism of the discharge depends on the polarity of the wire. For a positive wire electrons entering the high field region produce electron avalanches which maintain a highly ionized state near the wire. The positive ions produced by these avalanches drift towards the cathode under the influence of a decreasing field, and carry most of the current in the region outside the corona envelope. The remainder of the current is carried by electrons which are produced at the cathode or in the gas, mainly by photons from the discharge region.

In the case of a negative wire, the cathode is bombarded with high energy positive ions which produce the electrons necessary for a self sustaining discharge. These electrons move towards the anode and constitute the only current in the outer region. In general they form negative ions by attachment to neutrals.

Neglecting space charges the voltage V across such a system, with inner and outer cylinders of radii a and R respectively, is related to the field $E(a)$ at the surface of the inner cylinder by

$$V = E(a) a \ln (R/a) , \quad (1)$$

and as a first approximation, the voltage at which corona onset occurs may be obtained by equating $E(a)$ to the uniform breakdown field (approximately 3 MV/m for air at atmospheric pressure), but this is invalid for very small values of a . Peck¹² obtained an empirical equation for the field at the surface of the inner conductor necessary to produce visual ac corona,

$$E(a) = 3.1 m \delta [1 + 0.0974/\sqrt{(\delta a)}] \quad \text{peak MV/m} , \quad (2)$$

where δ is the relative air density ($\delta = 1$ at 25°C and 1.013 bar), a is in mm and m is an irregularity factor dependent on the condition of the wire ($m = 1$ for a polished wire).

In Appendix A the effect of space charge is also considered and the approximate relation between current i and voltage V for an established discharge

$$i \propto V(V - V') \quad \text{for } V \geq V' \quad (3)$$

is obtained, where V' is the critical voltage for onset of corona. This relation is based on the assumption that the current outside the discharge region is carried by ions of one sign only, and that the potential across the region of ionization is independent of current.

3 EXPERIMENTAL DETAILS

In search of the most suitable geometry for the discharge cell, preliminary experiments were performed with blade-plane and point-plane configurations, using a commercial razor blade and sewing needle respectively as the highly stressed electrode. The critical voltage for blades was several times higher than was to be expected¹³, being approximately 8 kV for a 10 mm gap. The point to plane configuration proved to be very sensitive to gap length and there was some evidence of corrosion resulting from the high current density at the point.

Therefore a coaxial arrangement was chosen in which a fine wire was suspended along the axis of a copper tube of 20 mm diameter and 100 mm length; guard rings were employed at each end. All of the experimental results quoted in this Report were obtained with 13 μ m diameter tungsten wire, unless otherwise stated.

The arrangement of the apparatus is illustrated schematically in Fig.1, which shows the discharge cell installed in a 300 mm diameter bell jar within a temperature controlled enclosure, thus facilitating control of both temperature and pressure.

Humidity control was achieved by creating a dynamic equilibrium state in which the rate of absorption of water vapour by a tray of silica gel was balanced by the rate of evaporation from the surface of a water bath. The effective surface area of the water bath could easily be varied by adjusting the water level in a conical funnel, thus controlling the rate of evaporation. The rate of absorption appeared to be related in some way to the water vapour pressure, and for different areas of water surface, equilibrium was established at different water vapour pressures. In this way values of humidity in the range* 0-90% RH were achieved.

* The measuring equipment was restricted to approximately 15-100% RH.

This system of control was implemented in a fairly simple fashion, which suffered the disadvantage that the water level could not be lowered if the pressure inside the bell jar was lower than atmospheric pressure by more than a few mbar; it was therefore possible to proceed only from low to high humidity. Also the presence of the absorber was undesirable when high humidity was required, but it would have been inconvenient to open the chamber and remove the tray, unless the temperature and pressure were approximately ambient. At low temperatures (5°C) the system became unstable and it was not possible to achieve a balance between emission and absorption (indicated by a steady measurement of dew point) over the full range of humidity.

As the chamber was completely sealed and of small volume, it was not possible to use a wet and dry bulb hygrometer for humidity calibration. Such instruments rely on evaporation of water and would therefore interfere with the control of humidity at low values. Consequently a Shaw 'Thermodew' humidity meter was used to provide a continuous indication of the dew point. This device senses changes in the intensity of light reflected from a mirror, and uses the information to control the mirror temperature by means of a Peltier cooling device. The mirror temperature is, in this way, made to oscillate about the dew point and is measured with a thermistor. To permit pressure variation the sensing head of the instrument was installed inside the bell jar.

The useful range of the meter is limited by the fact that the Peltier device can only cool the mirror to about 25°C below ambient temperature without additional cooling of the hot junction. Since the sensing head was enclosed in the chamber, such cooling was not practicable.

Both the 'Thermodew' and the discharge cell required ventilation to accommodate changing conditions in the chamber, and to remove products of the discharge from the corona cell. A fan drew a small sample of air through the 'Thermodew', while the discharge cell received the whole of the exhaust. A thermistor placed in the inlet to the fan, and connected in a bridge circuit, provided a continuous indication of temperature.

The high voltage supplied to the wire of the discharge cell was recorded on one axis of an X-Y plotting table by the method shown in Fig.2, while the current was recorded on the other axis. The resistance S comprises many resistors in series in a well ventilated container in order to minimise drift due to heating. To increase sensitivity in the voltage range of interest an offset voltage was applied to the input of the plotter. Expressions for this

voltage and the resulting sensitivity are given in Appendix B. For some readings a digital voltmeter was used to indicate voltage and current separately, no offset being necessary in this case.

4 RESULTS

4.1 Comparison with theory

For comparison with theoretical predictions, consider first the results obtained with dry air, using the wire as the anode throughout.

A set of typical current-voltage characteristics is shown in Fig.3, and an empirical relation was sought which describes such curves and the way they change with pressure. To a good approximation the relation

$$i = \alpha V(V - V')^\beta \quad (4)$$

holds, where V' is the critical voltage for onset of corona. The relationship (3) suggested that β should be unity, but the best agreement was obtained with $\beta = 1.2$, for a wide range of pressure.

The parameter α is of the form

$$\alpha = bp^{-1} + cp^{-2} \quad (5)$$

where at 26°C, b and c have the values

$$b = 2.4 \times 10^{-12}$$

$$c = -10^{-13}$$

if i is the current in amp and p the pressure in bar. No attempt was made to study the effect of temperature on these values.

The critical voltage V' is also strongly dependent on pressure, as is illustrated in Fig.4. The variation is reasonably well described by a relation of the form

$$V' = A p^{2/5} [1 + \mu \exp(-\nu p)] \quad (5)$$

which for pressures of the order of 1 bar is approximately

$$V' \propto p^{2/5} .$$

(Critical voltage is here taken as the voltage at which the discharge current suddenly increases to about 10^{-7} A.) This agrees quite well with Peek's relation (2) for visible corona onset, which under the same condition would reduce to

$$V' \propto p^{\frac{1}{2}},$$

although the criteria do not relate to exactly the same phenomenon.

4.2 The effect of humidity

Fig.4 also shows values of V' for humid air (relative humidity about 90%) at the same temperature. Over most of the pressure range considered the critical voltage is lower than for dry air; only at low pressure, where a change in the character of the discharge is to be expected, does this effect reverse.

Of primary interest, however, is the effect of humidity on discharge current, which is illustrated in Fig.5 for four wires of different diameter. In each case the temperature and total pressure were held at 20°C and 933 mbar respectively and the applied voltage at a convenient value for each wire. The curves show that the wires of larger diameter give greater sensitivity which, however, is obtained at the expense of linearity; the response at high humidity is approximately the same for all the wires but increases with wire diameter at low humidity.

Tungsten wires were used throughout, except for the smallest of these four, which was an alloy of platinum and tungsten.

4.3 The effect of temperature

Fig.6 illustrates the effect of temperature for a discharge in dry air and it can be seen that the sensitivity is linear up to at least 30°C . The corresponding curve for saturated air would be meaningless as an expression of temperature effect, since the saturation vapour pressure also changes with temperature. However, for the conditions considered the discharge current in saturated air varies very little with temperature, also the sensitivity of discharge current to water vapour pressure is approximately independent of temperature.

4.4 The effect of pressure

The discharge current is sensitive to pressure to a much greater extent than it is to temperature, as can be seen from the typical characteristics

displayed in Fig.3, and for this reason it is not practicable to present the effect of pressure on current at constant voltage explicitly, as was done for the effect of temperature. However, Fig.7 illustrates the relative change in current per unit change in pressure, for a range of pressure. This relative change is displayed for air of low and high humidity and can be seen to increase with decreasing pressure in both cases; in addition the two curves diverge at low pressure. This latter effect, illustrated more explicitly in Fig.8, is to be expected since the total pressure is approaching the magnitude of the water vapour pressure.

4.5 Polarity

All of the above results were obtained with positive wires, which proved to yield a more stable discharge and, as can be seen from Fig.9, a higher and more linear sensitivity to humidity. The sensitivity at high humidity is approximately the same for both polarities but the monotonic nature of the positive wire response is more suitable for measuring purposes.

5 DISCUSSION AND CONCLUSION

A study of corona loss from a 400 kV power transmission line by Bailey³ had shown an increase of discharge current with increasing water vapour pressure, while the effect is seen here to be a decrease. However, Bailey's work was carried out on conductors of about 50 mm diameter at much higher voltages than the present investigation, which might explain this apparent contradiction. Also, since Bailey's test line was in the open air, the effect of humidity may have been masked by the presence of water droplets on the conductor; the influence of weather generally on corona loss is discussed by Boulet and Jacubczyk⁴.

The present observation that the critical voltage is lowered by the presence of water vapour agrees with a similar observation by Waidmann, working with a pointed electrode; an explanation of the effect has been offered by Loeb¹⁴.

With regard to the application of the corona cell as a humidity meter, it is seen that a decrease in discharge current of at least 20% is available for a change in humidity from dry to saturated conditions and that the current/vapour pressure curve is approximately linear. For the bulk of this investigation a wire of 13 μ m diameter was used, but where enhanced sensitivity is required a wire of larger diameter could be employed. However, this modification entails the disadvantages of loss of linearity and the need for higher

voltages and more precise voltage regulation to offset the effect of an increase in $\frac{di}{dV}$.

In a practical instrument the side effects of temperature and pressure would necessitate some form of compensation. Twin cells, one in a stream of ambient air and the other in a stream of dried air, can be employed if the temperature and pressure are maintained at the same values in each cell. This condition might be difficult to achieve unless the temperatures of both cells were raised to the same (constant) value, and an increase in response time will be inevitable.

Alternatively, environmental temperatures and pressures can be measured independently and the corrected humidity obtained by computation from calibration data. The range of conditions considered so far is necessarily limited but is sufficient to indicate that the sensitivity of discharge current to water vapour pressure will not seriously decrease from 1%/mbar at pressures above atmospheric, and is almost independent of temperature; a more complete calibration would include conditions of higher pressure and temperature likely to be encountered in industrial processes.

It is not clear why other electrode configurations, particularly the blade-plane arrangement, proved to be unsatisfactory. In a practical device, where robustness is important, a blade offers considerable advantages and further investigation of this aspect may be rewarding. The results obtained with the coaxial arrangement, however, suggest that the corona cell could form the basis of a simple and inexpensive humidity meter with a linear response and an accuracy of better than 5% RH depending on the power supply and current measuring equipment used, and also on the efficiency of temperature and pressure compensation techniques. The range of the device could only be tested from about 15% to 85% RH with the calibration equipment employed, but did not appear to be limited at either low or high humidity.

In principle the cell described in this Report could have a response time of the order of the transit time for an ion across the cell (about 200 μ s), although the practical limit is likely to be imposed by ventilation requirements. This difficulty could be minimised by decreasing the size of the cell, but would necessitate a smaller wire, which would be more fragile, and lower current. However in its present form the cell compares favourably with infra-red absorption devices regarding response time and has the additional advantage of simplicity and low cost.

The instrument will lend itself most readily to control of processes in which temperature and pressure are maintained within close tolerances. In such applications the need for physical compensation techniques will be removed and any adjustment required can be easily applied electronically without deterioration of the inherently high response rate of the instrument.

Appendix A

THE CURRENT-VOLTAGE RELATION

Once the discharge is established we can consider the gap in two parts, with the boundary defined by radius r_0 .

In the region $a < r < r_0$, in which ionization occurs, there is no net space charge, and we have from Poisson's equation

$$\frac{d}{dr} [E(r)r] = 0$$

where $E(r)$ is the electric field strength at radius r .

Beyond the glow discharge, i.e. in the region $r_0 < r < R$ we can assume that the current is carried by ions of one sign, then the current per unit length is

$$i = 2\pi r \rho v$$

where v is the radial velocity and ρ the charge density of ions at radius r . Writing K for the mobility of the ions we have

$$\rho = \frac{i}{2\pi r K E}$$

and substituting in Poisson's equation

$$\frac{1}{r} \frac{d}{dr} (E r) = \frac{\rho}{\epsilon_0} = \frac{i}{2\pi \epsilon_0 K E r},$$

which, on integration, becomes

$$(E r)^2 = \frac{i}{2\pi \epsilon_0 K} r^2 + C.$$

If E_0 is the field at radius r_0 , we can write approximately

$$C = (E_0 r_0)^2.$$

The potential in this region satisfies

$$\frac{dV}{dr} = \frac{1}{r} \left[\frac{i}{2\pi \epsilon_0 K} r^2 + C \right]^{\frac{1}{2}}$$

and integration between r_0 and R yields the potential difference across this part of the gap,

$$\begin{aligned} V(r_0) &= \left[\frac{i}{2\pi \epsilon_0 K} R^2 + C \right]^{\frac{1}{2}} - \left[\frac{i}{2\pi \epsilon_0 K} r_0^2 + C \right]^{\frac{1}{2}} \\ &+ \frac{1}{2} C^{\frac{1}{2}} \ln \left(\left(\left[\frac{i}{2\pi \epsilon_0 K} R^2 + C \right]^{\frac{1}{2}} - C^{\frac{1}{2}} \right) \left(\left[\frac{i}{2\pi \epsilon_0 K} R^2 + C \right]^{\frac{1}{2}} + C^{\frac{1}{2}} \right)^{-1} \right) \\ &- \frac{1}{2} C^{\frac{1}{2}} \ln \left(\left(\left[\frac{i}{2\pi \epsilon_0 K} r_0^2 + C \right]^{\frac{1}{2}} - C^{\frac{1}{2}} \right) \left(\left[\frac{i}{2\pi \epsilon_0 K} r_0^2 + C \right]^{\frac{1}{2}} + C^{\frac{1}{2}} \right)^{-1} \right) . \end{aligned}$$

This expression may be simplified for small current by expanding in powers of i and neglecting terms of second and higher orders, hence

$$V(r_0) = \sqrt{C} \ln \frac{R}{r_0} + \frac{i R^2}{8\pi \epsilon_0 K \sqrt{C}} .$$

From the behaviour of uniform field discharges, it is reasonable to assume that the potential across the region of ionization is fairly independent of R and i , so the potential across the whole gap becomes

$$V = V' + \frac{i R^2}{8\pi \epsilon_0 K \sqrt{C}}$$

where V' is the total voltage for zero current, i.e. the critical voltage for onset of corona.

Substituting

$$\sqrt{C} = E_0 r_0$$

and assuming that $E_0 r_0$ is not perturbed by the space charge in the region $r_0 < r < R$, we write

$$E_0 r_0 = V / \ln (R/a)$$

which gives finally

$$i = \frac{8\pi \epsilon_0 K}{R^2 \ln (R/a)} V(V - V') .$$

Appendix B

OFFSET VOLTAGE AND PLOTTER SENSITIVITY

In order to display on the plotter only the voltage range of interest it was necessary to offset the signal with a voltage V_1 . Let V_0 be the value of the applied voltage for which the plotter input is zero. Referring to Fig.2 we see that

$$V_0 = \frac{(S + s)V_1}{s} \approx \frac{S V_1}{s} .$$

The currents I flowing through S , and I_1 through the plotter input resistance σ , are related by

$$V = I S + (I - I_1)s$$

and

$$s(I - I_1) = V_1 + I_1 \sigma$$

which combine to give

$$V - V_0 = I_1 [S(s + \sigma) + s\sigma]/s .$$

Since $\sigma \ll S$ and $s \ll S$ the required sensitivity becomes

$$\frac{I_1}{V - V_0} = \frac{s}{S(s + \sigma)} .$$

REFERENCES

<u>No.</u>	<u>Author</u>	<u>Title, etc.</u>
1	L. B. Loeb	Electrical coronas. University of California Press, Berkeley and Los Angeles (1965)
2	L. B. Loeb	Handb. d. Phys. (S. Flügge, Ed.) Vol.XXII, p.445, Springer, Berlin (1956)
3	B. M. Bailey	I.E.E.E. Trans. Vol. PAS-86, 1141 (1967)
4	L. Boulet B. J. Jakubczyk	Trans. Eng. Inst. Canada, Paper EIC-64-ELEC 4, July 1964
5	C. C. Francisco D. J. Beaubien	Humidity and moisture. (A. Wexler, Ed.) Vol.1, p.165, Reinold, New York (1965)
6	S. H. Jury L. P. Bosanquet Y. W. Kim	Rev. Sci. Inst., <u>38</u> , 1634 (1967)
7	J. R. Lai G. M. Hidy	Rev. Sci. Inst., <u>39</u> , 1197 (1968)
8	A. C. Jason	Humidity and moisture. (A. Wexler, Ed.) Vol.1, p.372, Reinold, New York (1965)
9	D. T. Gjessing et al.	Journal of Physics E, ser. 2, <u>1</u> , 107 (1968)
10	J. Sargent	Rev. Sci. Inst. <u>30</u> , 348 (1959)
11	R. C. Wood	Humidity and moisture. (A. Wexler, Ed.) Vol.1, p.492, Reinold, New York (1965)
12	F. W. Peek, Jr.	Dielectric phenomena in high voltage. Engineering, p.66, McGraw Hill, New York (1915)
13	J. M. Gilliland B. W. Viney	Electric fields at the surfaces of fine wires and sharp edges. R.A.E. Technical Report 68271 (1968)
14	L. B. Loeb	Ref.1, p.225

Fig. 1

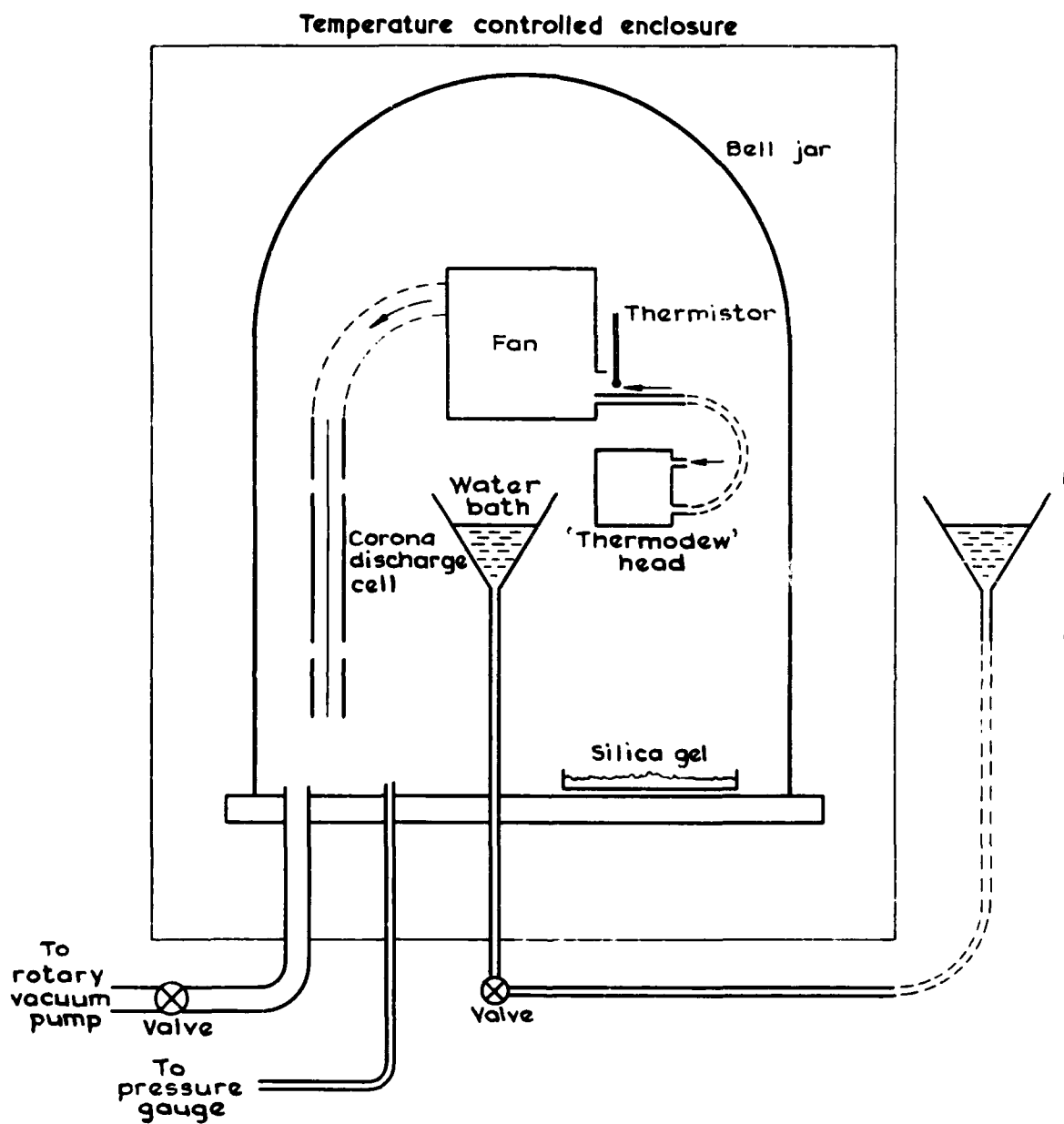


Fig.1 Test chamber for corona discharge cell

TR. 70106

054 900614

Fig. 2

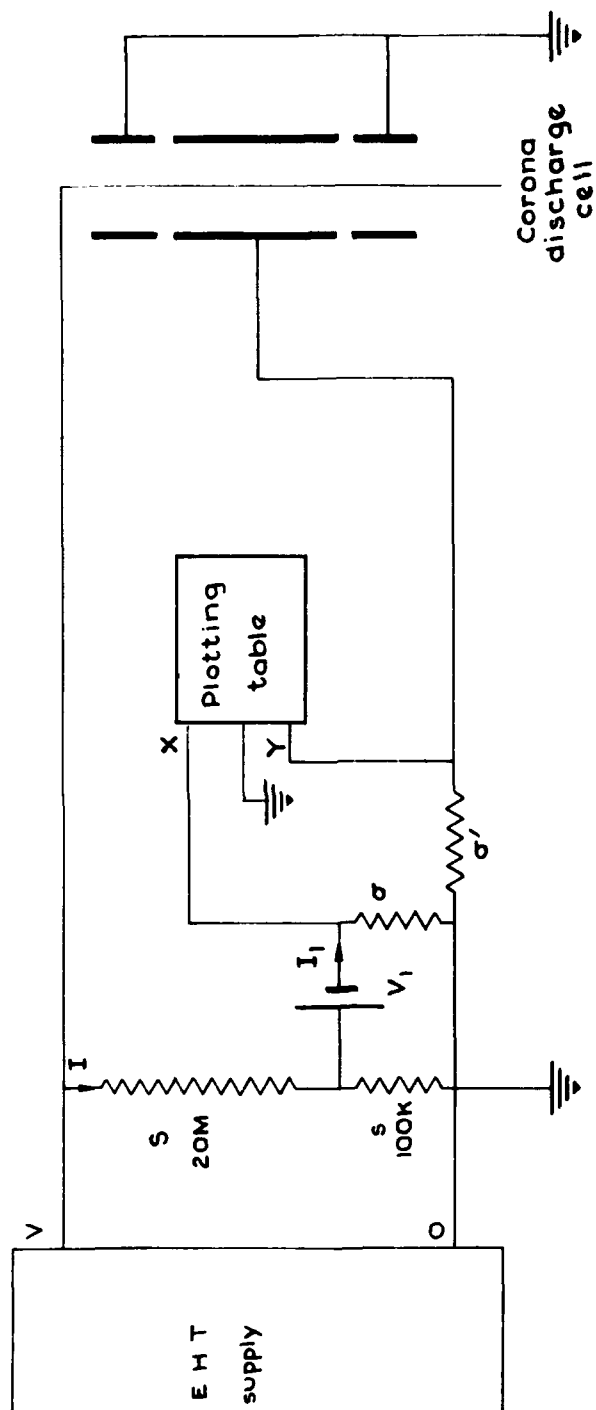


Fig.2 Discharge voltage /current measuring circuit

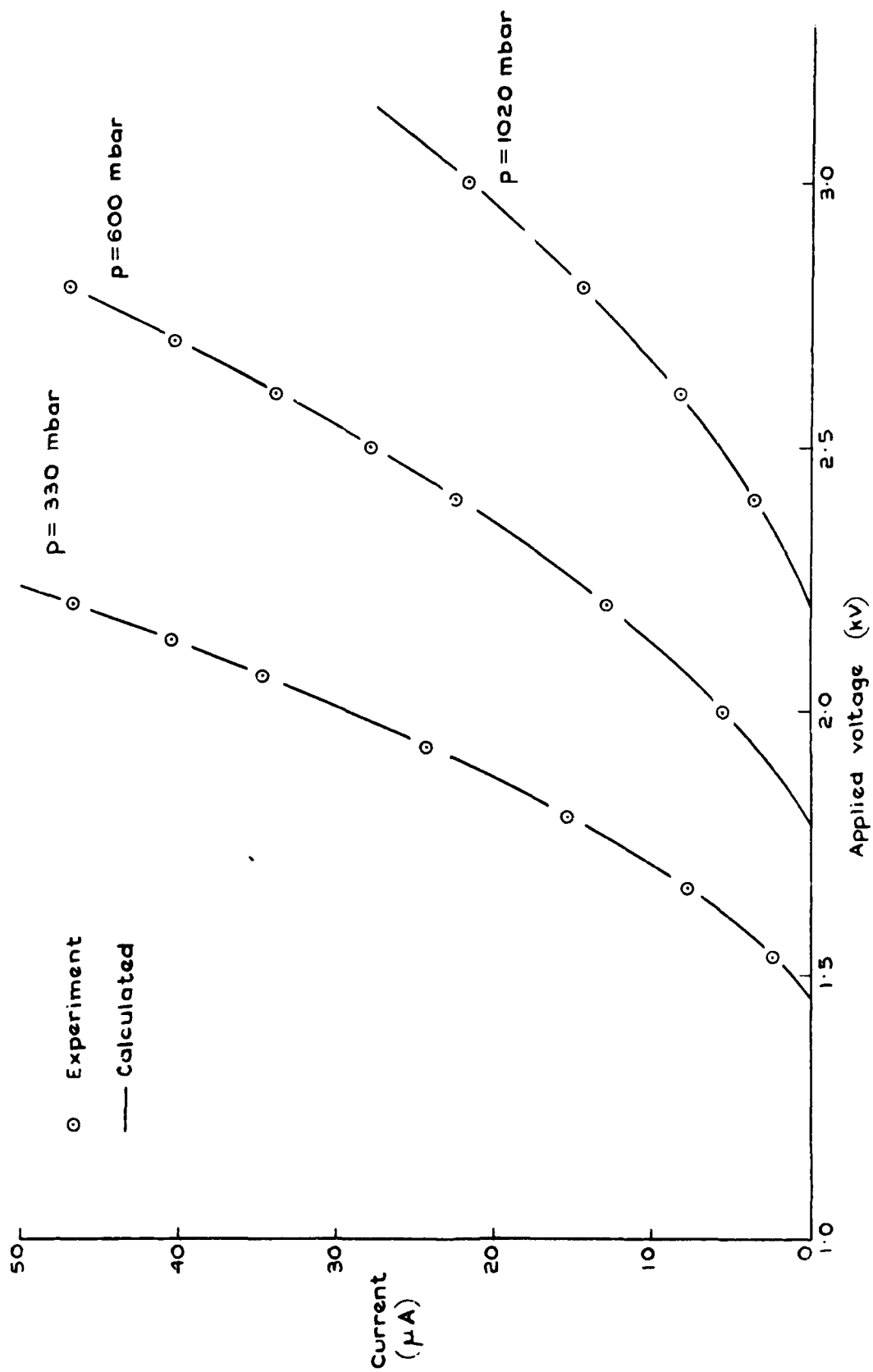


Fig. 3

Fig. 3 Typical discharge characteristics in dry air at 26°C

Fig. 4

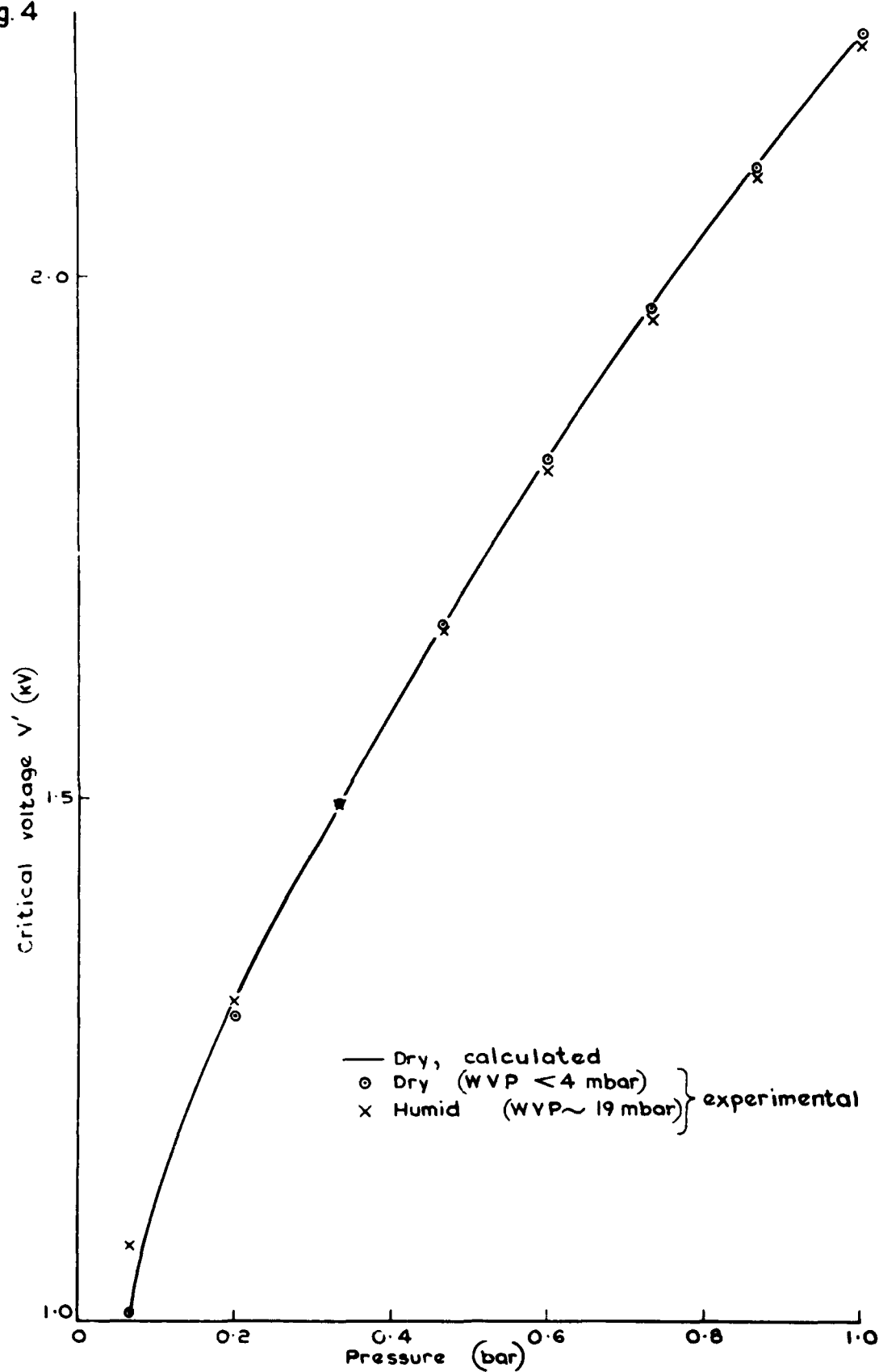


Fig. 4 Effect of pressure on critical voltage at 19°C

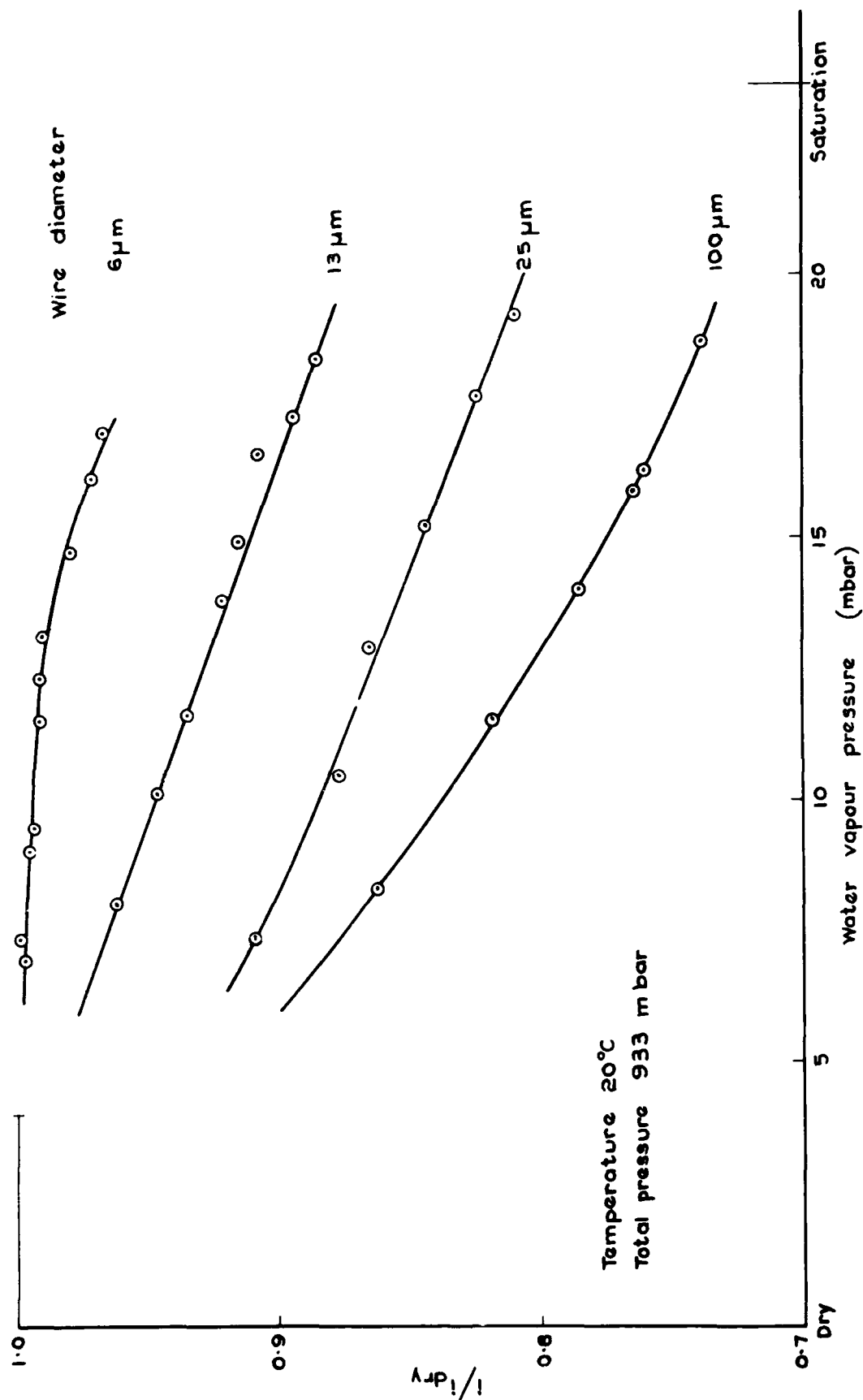


Fig. 5 Effect of humidity on discharge current

Fig. 6

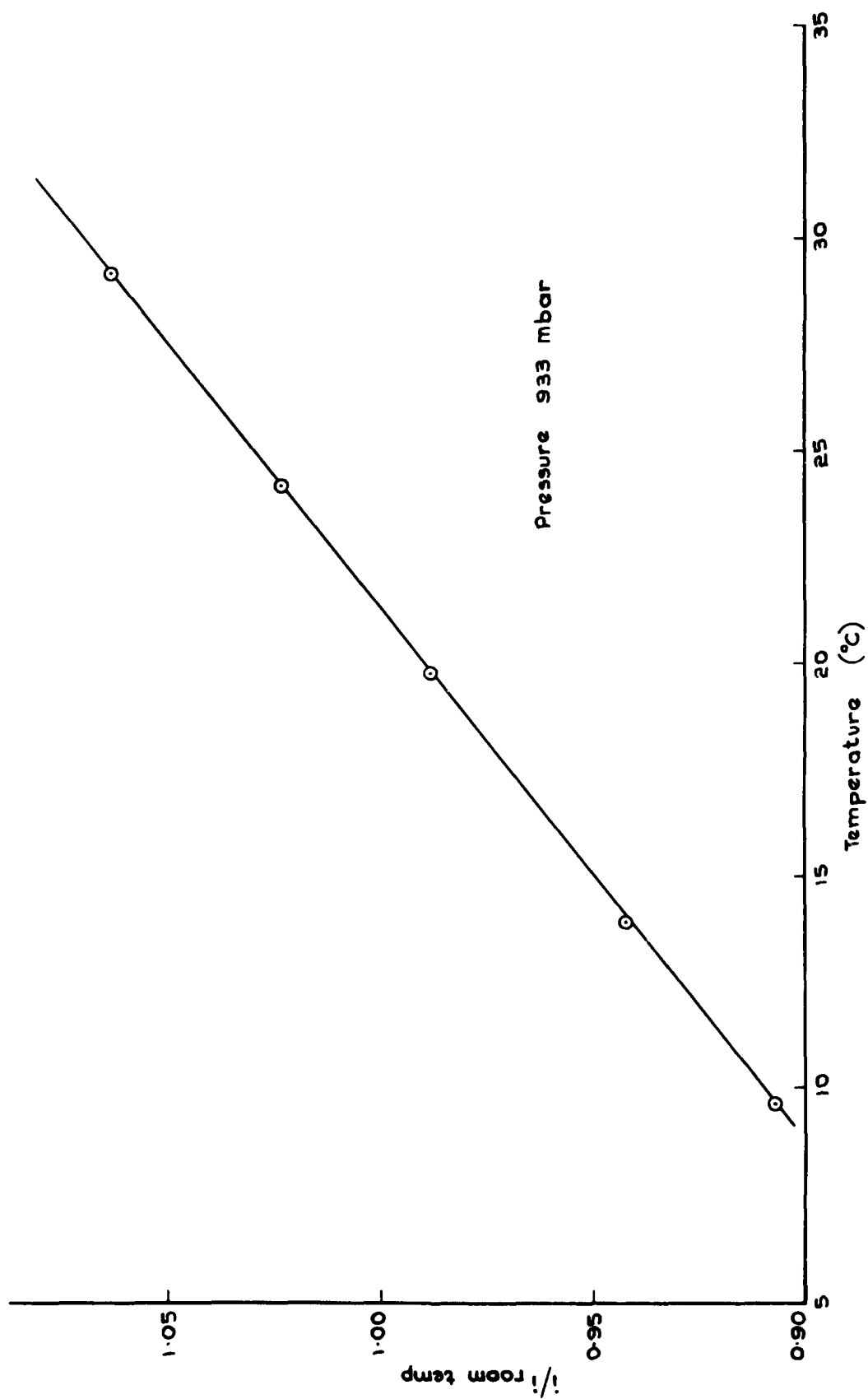


Fig. 6 Effect of temperature on discharge current

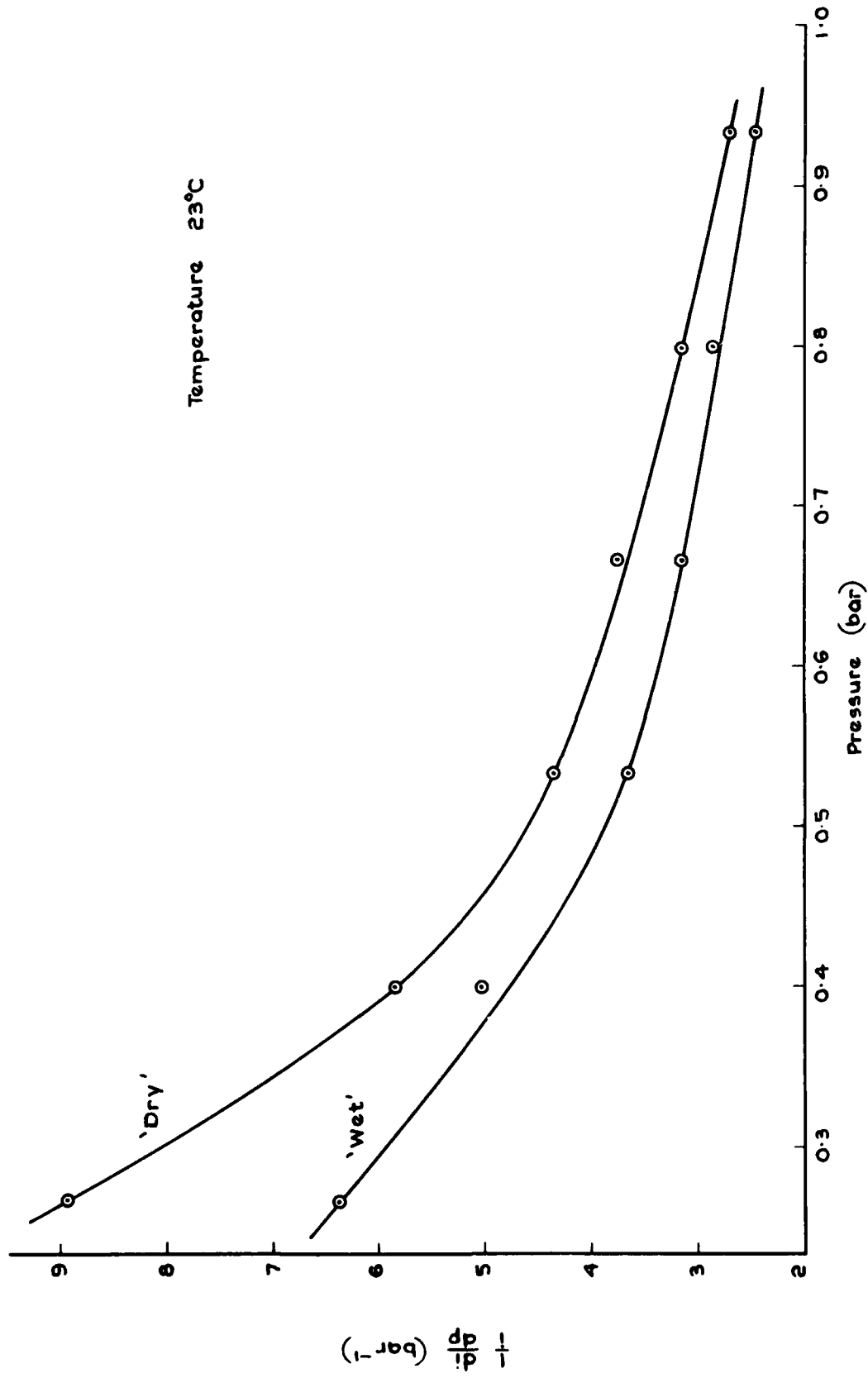


Fig. 7

Fig. 7 Sensitivity of discharge current to pressure

Fig.8

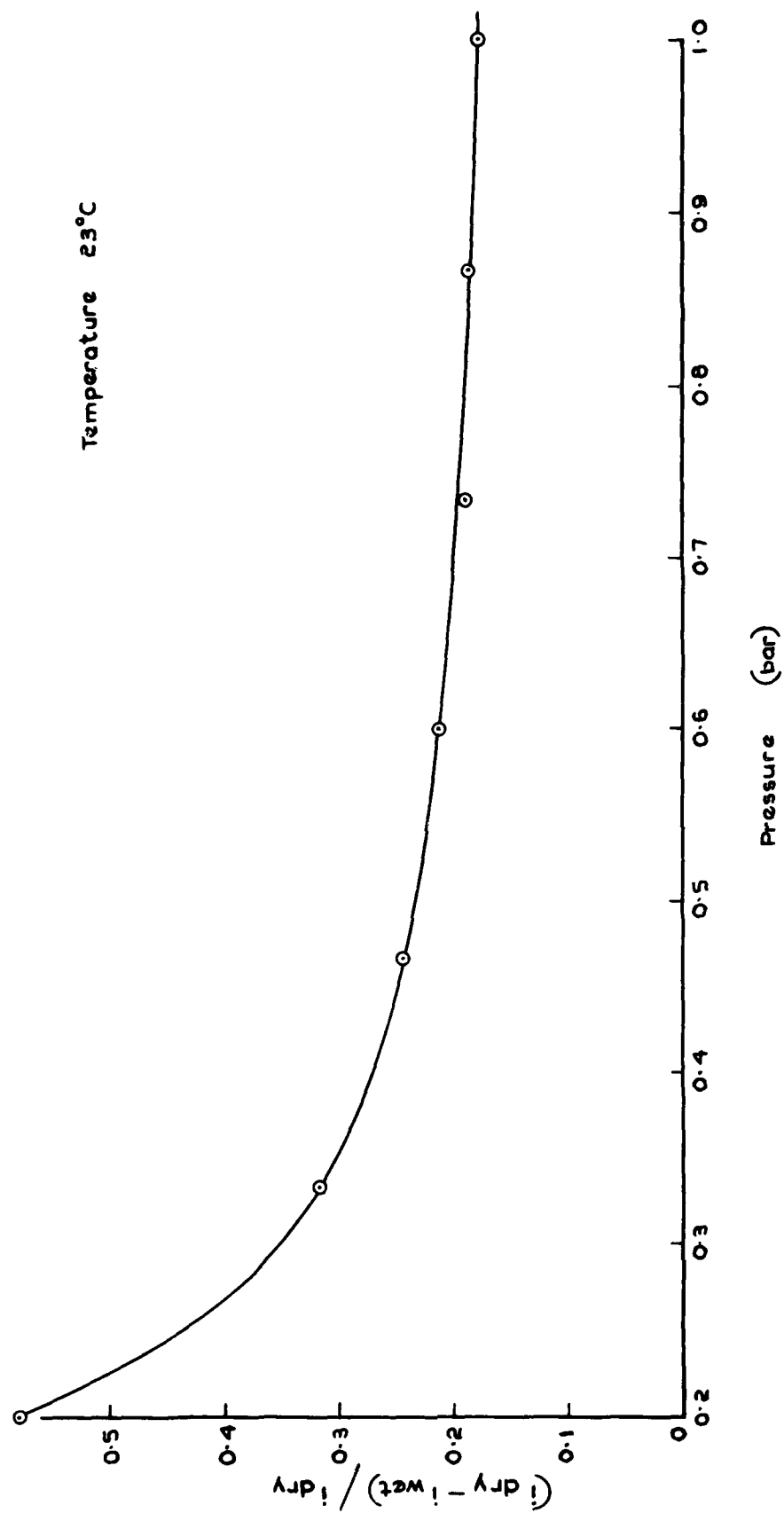


Fig. 8 Effect of pressure on sensitivity to humidity

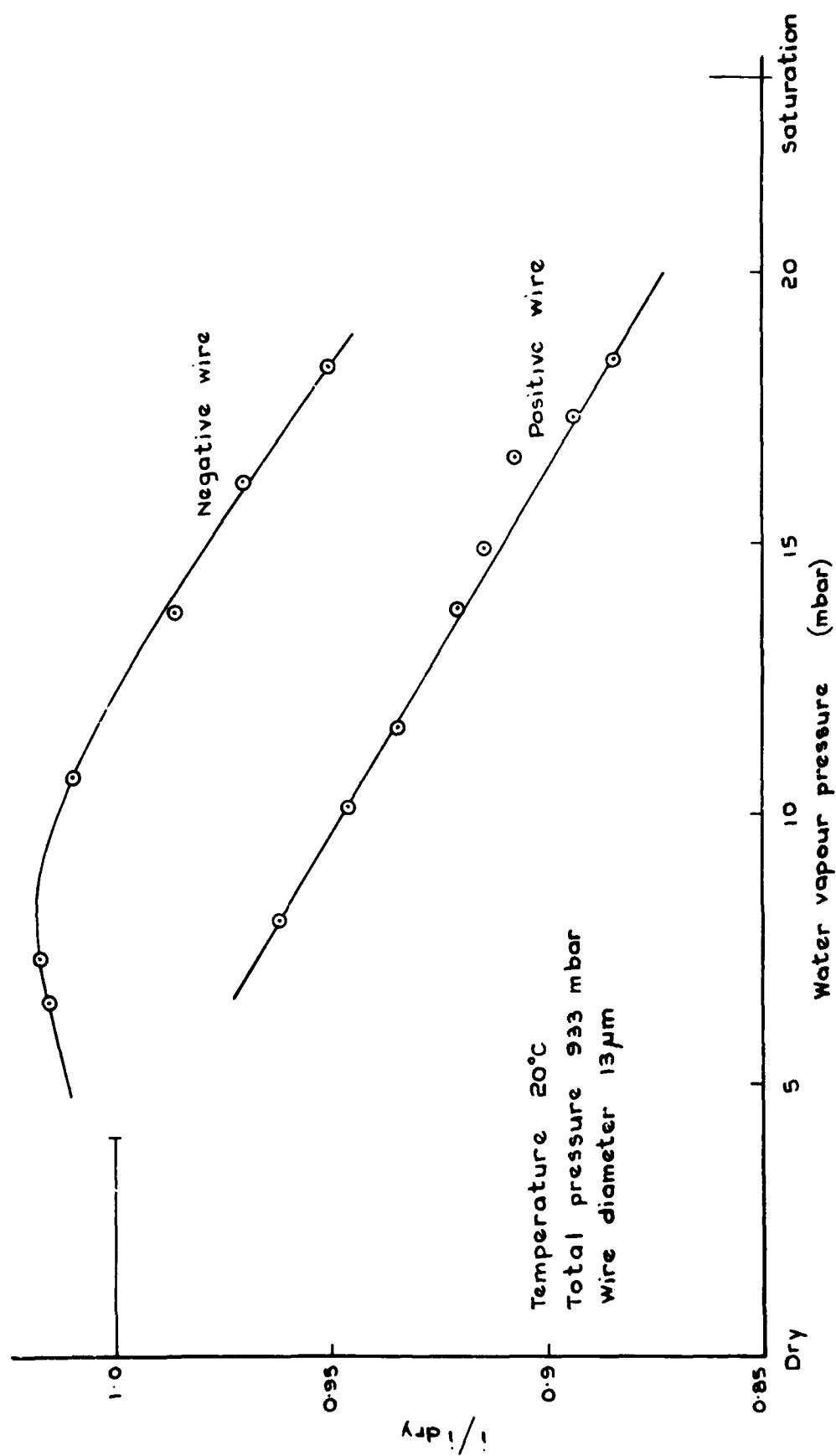


Fig. 9

Fig. 9 Comparison of positive and negative wires